JOURNAL OF MECHANICS OF CONTINUA AND MATHEMATICAL SCIENCES
www.journalimcms.org

ISSN (Online) : 2454 -7190 Vol.-15, No.-2, February (2020) pp 70-83 ISSN (Print) 0973-8975

SHORT TERM RAIN FORECASTING FROM RADIOMETRIC BRIGHTNESS TEMPERATURE DATA

Kausik Bhattacharyya[1], Manabendra Maiti [2], Salil Kumar Biswas[3], Md Anoarul Islam[4], Ayan Kanti Pradhan[5], Pradip Kumar Ghosh[6], Judhajit Sanyal[7]

[1]Department of Physics, Tamralipta Mahavidyalaya, Tamluk, East Medinipur, West Bengal 721636, India

[2]Department of Electronics & Communication Engineering, Techno International New Town, DG 1/1, Action Area I, Newtown, Kolkata, West Bengal 700156, India

[3]Department of Physics, University of Calcutta, 92, AcharyaPrafulla Chandra Road, Kolkata, West Bengal 700009, India

[4]Department of Electronics & Communication Engineering, Techno International New Town, DG 1/1, Action Area I, Newtown, Kolkata, West Bengal 700156, India

[5]Department of Electronics, Acharya Prafulla Chandra College, New Barrackpore, North 24 Parganas, Kolkata, West Bengal 700131, India

[6]Department of Electronics & Communication Engineering, Techno International New Town, DG 1/1, Action Area I, Newtown, Kolkata, West Bengal 700156, India

[7]Department of Electronics & Communication Engineering, Techno International New Town, DG 1/1, Action Area I, Newtown, Kolkata, West Bengal 700156, India

[1]kausikbh@gmail.com,[2]manab1972@yahoo.com, [3]skbiswas23@gmail.com, [4]mdanoarul@gmail.com, [5]ayanpradhan@yahoo.co.in, [6]pradip.ghosh@tict.edu.in, [7]sanyaljudhajit@gmail.com

Corresponding Author: Manabendra Maiti

https://doi.org/10.26782/jmcms.2020.02.00007

Abstract

Prediction of rainfall is important in terms of the impact of a rain event on various systems such as communication systems. Traditional approaches used to predict rain events are often sensitive to fluctuations in the datasets on which the predictions are made. The present paper therefore develops a robust machine learning based technique for accurate short term rain forecasting, based on

experimentally collected data. Ground based microwave radiometer allows continuous monitoring of ambient temperature, water vapour and liquid water, and other hydrometeors through measurement of radiometric brightness temperature at different frequencies in clear and cloudy weather conditions. The radiometric brightness temperature outputs at 23.834 and 30 GHz are used to establish a relation where data trends which are precursors to rain events can be identified using this parameter. Spline equations are modeled by partitioning the dataset. The predictability of the occurrence of precipitation and the rainfall intensity has been studied based on the rise of brightness temperature from clear to cloudy weather conditions. The rise of brightness temperature at 23.834 and 30 GHz show that the precursory variations of this parameter preceding rain events are observable from 29 to 47 minutes prior to precipitation depending upon the nature of rainfall patterns. The data collected empirically displays trends that are used in this paper to provide a clear forecast of short term precipitation. Spline regression based machine learning models incorporating monthly trends, proposed in this paper improve the accuracy of prediction of short term rain events.

Keywords: Radiometer, brightness temperature, microwave, propagation, rain, weather forecasting

I. Introduction

Radiometric measurements are nowadays becoming more and more interesting from the perspective of analysis of different atmospheric phenomena [XXV] [XV], weather monitoring and short term weather forecasting etc. The early experiments on radar reflectivity, and temperature and humidity profiles by radiosonde measurements [XXI] [X] [XX] [XVII] are now performable by the microwave radiometer as it can monitor the atmosphere continuously, thus ensuring that the data obtained can be used for design of more accurate predictive models for the atmosphere.

The continuous radiometric measurements hold an edge over radiosonde measurements as the latter is made twice daily. A system incorporating a ground-based microwave radiometer needs to consider the electromagnetic interaction between the microwave radiation and the medium concerned since radiometric response depends on the various radiative sources along the propagation path.

However the accuracy depends on the atmospheric inhomogeneity due to hydrometeors in different phases. The authors in [XXVI] made it clear that the brightness temperature given by the ground-based radiometer is under scatter free condition. However to observe the atmosphere continuously for various advantageous reasons for retrieval of geophysical observables, such as the total amount of water vapor (PWV), the non-precipitating cloud liquid content (LWC) and the zenith wet delay (ZWD). Radiometric measurement is the only answer for short-term weather forecasting and air pollution monitoring due to its all-weather capability.

Communication systems are nowadays facing challenges to meet the needs of higher rate of data transfer in microwave and millimeter wave frequency bands from over 10

GHz to 300 GHz. This necessitates knowing the behavior of a microwave signal in this frequency range while passing through atmosphere. The signals in the microwave/millimeter wave bands interact badly with water vapor, rain, hydrometeors in different phases and many other gaseous constituents and aerosols. Near the surface of the Earth, the atmospheric constituents are mostly present due to gravity, and prominent signal fading is observed here.

Moreover the impairment of electromagnetic signals above 10 GHz by the dynamic weather conditions such as rain [IX] necessitates the development of ideas and techniques to predict future rain events because rain drops absorb and scatter radio waves leading to signal gain reduction [XXII].Some scholars [XXVII] compared radiometric profiles with radiosonde data and forecasted sounding in the evaluation of accuracy of radiometer temperature and water vapor soundings. Scholars in [XXVII] described a case study showing the improvement of forecasting on the basis of variation in assimilation of radiometric soundings. Researchers in [V] presented the application of an instability index derived from radiometric studies for the nowcasting of heavy rainfall and thunderstorms in Hong Kong. [VI]and[VII] described the need of radiometer for now casting. [XVIII]showsa feasibility study of nowcasting convective activity in Gadanki (13^0N, 79.2^0E).

Scholars [II] retrieved the integrated water vapour and the liquid water content by using radiometric data in Italy. Researchers in [VIII] also used radiometric output to examine the differences in cloud liquid water path at a coastal and at an inland location on the north slopes of Alaska. Scholars in [XXVIII] also measured the water vapour content and compared with radiosonde observations in USA. [XVI] also used radiometric data for rainfall prediction. [III] and [IV]present analysis of radiometric data at Cabauw (NL) in May-July 2009 and in April 2008 to check sky status. [XIV] illustrates a model for finding the integrated water vapour content and non-precipitable cloud liquid water over Brazil exploiting a multifrequency microwave radiometric method and compared the results with those obtained by radiosonde data analyses. [XI], [XII] and [XIII] described a parameter based on liquid water content and water vapour content in the two hour period before raining. These findings prompted the present authors to make a comprehensive study for short term local precipitation forecast by using brightness temperature records of a microwave radiometer from two hours before for seven successive months from January to July of 2009 at Cauchoeria Paulista (22.57^0 S, 89^0 W), Brazil . In this context researchers [XVI] used radiometric data to establish an algorithm for the estimation of rainfall intensity and to fix the optimal time period for its comparison with corresponding rain gauge data.

In recent years, deep learning techniques have been used for estimation of rainfall [XXIII]. The prediction of rain attenuation has also been carried out in [I] using back propagation neural networks (BNNs), with an acceptable correlation coefficient tending to 0.83 indicating the statistical relationship between rain attenuation and rain rate for the proposed model. Some recent researches have proposed a simple now casting algorithm for short-term prediction of rainfall based on GPS signal data [XIX]. Others [XXIV] have used Bayesian Artificial Neural Networks to predict cumulative rainfall time series data.

Combinations of different machine learning techniques and algorithms have also been favoured by some researchers since such approaches help to overcome the drawbacks of many standard machine learning algorithms. For example, some researchers [XXIX] have endeavoured to design a multilayer perceptron based machine learning model which incorporates variations of physical factors ignored by many standard machine learning algorithms that predict rain events. Such machine learning based approaches to rainfall prediction have gained popularity in recent years due to their high accuracy and ability to work with high volumes of data. The current paper consequently uses machine learning to enhance the accuracy of prediction of rainfall in the context of short term prediction of rain events, through the application of spline regression on the experimentally collected data.

II. Theoretical Background and Experimental Data Analysis

A microwave radiometer observes the radiation intensity at a number of frequencies out of which 23.834 GHz and 30GHz are chosen because 23.834 GHz appears to be independent of pressure broadening and the other frequency is the water vapor absorption minima in the microwave spectrum. It has also been found that selection of this frequency pair for the measurement of vapor and liquid is optimal [XIV].

It is to be mentioned here that microwave radiometer profiler manufactured by Radiometrics Corporation has been used for the purpose of temperature and water vapour profiling. This radiometer provides temperature and humidity soundings and also cloud liquid. This profiler includes a vertical infrared sensor and surface temperature, humidity and pressure sensor. On the other hand, the disdrometer records drop size distribution and hence the rainfall intensity as well. Data collection was carried out from January to July during 2009 in Brazil including the occurrence of rain and counted for about 2 minute intervals. According to authors in [XI], [XII] and [XIII], if a rain event occurs in the interval of two hours after the termination of the previous rain event then both are assumed to be the same rain event. When the time interval of difference of the brightness temperature T_B is chosen to be shorter than two hours, accurate prediction of precipitation for the succeeding event could not be ensured. If a longer interval than two hours is considered, only a few number of rain events are identifiable and these are usable for our study. But we have restrained ourselves within the interval time of two hours for the prediction of rain events. Two data sets, one being the rain records and the other one being the non-rainy records were used to examine the change of brightness temperature before raining to carefully eliminate the seasonal dependence and weekly cyclical variations of both the data sets and the non-rainy records were selected in tune with the same time period after a week. Then the brightness temperature data were excluded from the non rainy record if it had rained during the two hours interval to ensure that the non-rainy record had no relation with rain. Using this idea the samples have been found to number more than 100 pertaining to rain records and 220 pertaining to non-rainy records from January 2009 through July 2009 in Cachoeira Paulista (22^0 South), Brazil.

The time series of surface temperature, relative humidity and rain rate at the instrument site on 22nd March, 2009, during a five hour period is presented in Fig. 1,

for the sake of clarity. It is interesting to note that the temperature starts falling from 299.05 K to 294.69K within about 95 minutes before rain starts. On the other hand, the relative humidity attains its maximum value of about 97.96 % just before rain starts. This statement is in conjunction with the observations from Fig. 1 where the rain rate profile is shown for the same time period.

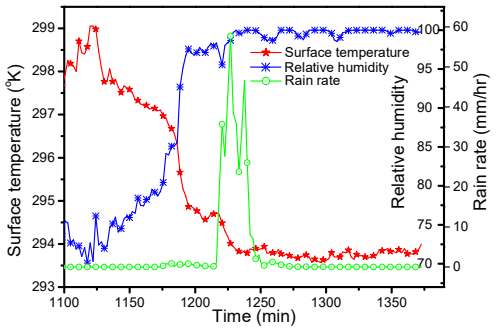

Fig. 1: Time series of temperature, relative humidity and rain rate at the instrument site levels, on 22 March 2009 in Brazil

Here for the sake of calculation, the brightness temperature two hours before the start of the rain event is taken as reference value. The difference between the current and reference value is used here. In Fig. 2, a plot of time series of all these values of difference of T_B (K) between current and reference values at 23.834 and 30 GHz versus rain rate (mm/hr) illustrates that the rising tendency of brightness temperature difference for these two frequencies reaches the values 80K and 100K at the respective frequencies till the rain event ensues.

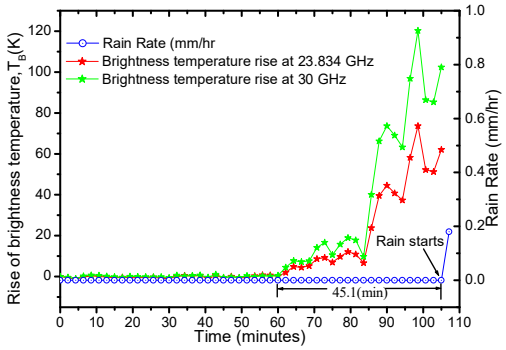

Fig. 2: Time series representation of Rise of brightness temperature on 31 March, 2009 for a particular rain event

The time gap of 45 (approx) minutes calculated from Fig. 2 corresponds to the difference of time from the sign of rising tendency of T_B (K) difference till the start of rain event. Table 1 is presented here depicting the occurrence of rain events with brightness temperature data at the given frequencies, at some calculated time gaps before rain for events occurring in the months from January to July, 2009 in Brazil. This time gap is considered a diagnostic tool for nowcasting of rain at least half an

hour or above. So it may be conclusively mentioned that the rising tendency of T_B (K) difference is a precursor to rainfall.

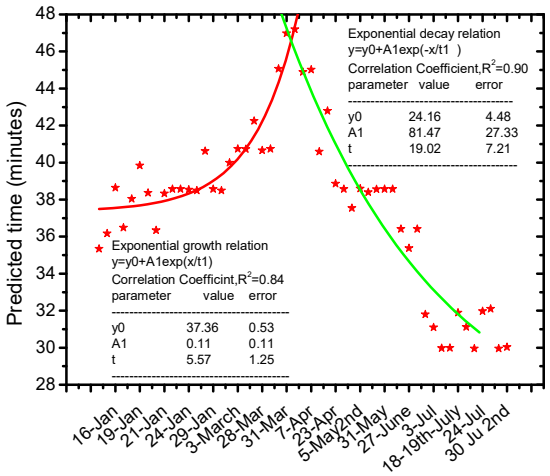

Fig. 3: Rain prediction time at different months of the year 2009 over Brazil

Table 1:Values of brightness temperature at 23.834 and 30 GHz and rain precursor time

Sl. No. of events	Dates of the year 2009	Reference value of T_B (K) at 23.834GHz	Reference Value of T_B (K) at 30GHz	Precursor time of rain event (minutes)
1	14th Jan	70.26	30.80	35.58
2	15th Jan	68.15	30.25	36.18
3	16-17th Jan	72.23	33.58	38.65
4	17th Jan	73.04	31.75	36.49
5	18th Jan	68.8	30. 43	38.05
6	19th Jan	77.99	38.17	39.85
7	20th Jan 1st spell	75.6	34.9	38.37
8	20th Jan 2nd spell	76.48	34.6	38.43
9	21th Jan	77.39	37.28	38.34
10	22th Jan	77.44	39.70	38.58
11	23th Jan	75.89	42.17	38.56
12	24th Jan	70.66	32.13	38.54
13	26th Jan	76.16	36.9	38.5
14	28th Jan	78.19	35.42	40.63
15	29th Jan	78.4	37.5	38.58
16	30th Jan	74.07	34.12	44.90
17	2nd Feb	73.50	33.71	40
18	3rd Mar	70.76	30.85	40.74
19	18th Mar	72.13	30. 25	40.73
20	22nd Mar	71.66	29.24	42.26
21	28th Mar	78.51	38.84	40.66
22	29th Mar	73.17	31.4	40.74
23	30th Mar	72.4	30.04	45.07
24	31st Mar	70.73	29.51	44.99
25	5th April	76.64	39.54	47.20
26	6th April	81.11	46.79	44.9
27	7th April	73.19	31.53	45.02
28	13th April	72.43	32.22	40.59
29	15th April	62.49	30.84	42.80

30	23rd April	54.62	21.9	38.86
31	4th May	54.01	21.98	38.58
32	5th May 1st spell	54.18	22.94	37.55
33	5th May 2nd spell	46.7	19.52	38.60
34	28th May	62.73	25.29	38.40
35	29th May 2nd spell	71.3	42.31	38.57
36	31st May	61.9	24.3	38.58
37	1st June	52.33	20.84	38.58
38	5th June	39.91	16.14	36.42
39	27th June 1st spell	54.76	23.86	35.38
40	27th June 2nd spell	54.94	21.76	36.42
41	2nd July	47.13	32.84	31.81
42	3rd July	54.70	23.91	31.10
43	10th July	47.37	18.52	29.98
44	11th July	63.34	29.62	30
45	18-19th July	53.65	23.45	31.90
46	22nd July	42.84	17.08	31.12
47	23rd July	58.54	26.42	29.96
48	24th July	64.95	30.17	31.98
49	28th July	60.09	24.24	32.11
50	30th July 1st spell	51.49	25..9	29.96
51	30th July 2nd spell	58.48	26.8	30.04

The variation of precursor times for rain events is shown in the preceding Table 1, with respect to reference brightness temperatures measured at two frequencies, namely 23.834 GHz and 30 GHz. Measurements are taken for the months from January to July. Multiple rain events have been observed on some of these dates, which can be seen from the table. Additionally, only one rain event has been recorded in February. It is clear from the above Table 1 that the precursor time of rain event ranges from 29 to 47 minutes depending upon the season concerned. It is noticeably found that at pre & post monsoon season this time gap is less than the monsoon period which is pictorially present in Fig. 3. From Fig. 3 it is clear that the precursor time is increasing from January and attains its peak value at April. It is in conjunction with the monsoon activity in this location. In Brazil monsoon season starts from January and ends at April.

An attempt has been made to carry out regression analyses (Fig. 3) for rain prediction time in pre-monsoon and post-monsoon periods yields the following best-fit relations along with correlation coefficient, R. The pre-monsoon period rain prediction time variation has a trend of exponential growth while the post-monsoon period shows exponential decay in the rain prediction time T_{RP}.

$$T_{RP}(\text{Pre}-\text{monsoon}) = 37.36 + 0.11 * e^{\text{months}/5.57} \text{ with correlation, R2} = 0.84 \quad (1)$$

$$T_{RP}(\text{Post monsoon}) = 24.16 + 81.47 * e^{-\text{months}/19.02} \text{ with correlation, R2} = 0.90 \quad (2)$$

Another interesting point is to be noted here that the highest precursor time, 47 minutes is seen on 5th April 2009 which was also the maximum rain rate day throughout the year.

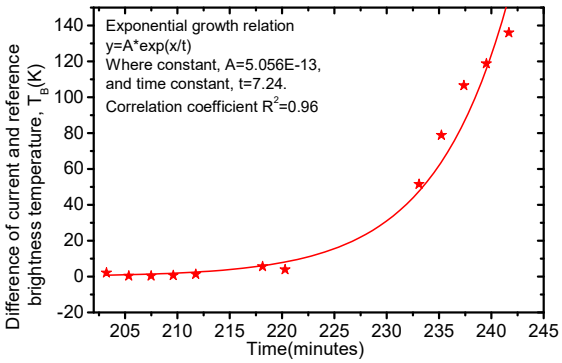

Fig. 4: Change of brightness temperature from reference value on 19th January, 2009

The nature of the rising tendency of brightness temperature of a precipitation event on 19th January is shown in Fig. 4. The relationship between the difference in brightness temperature and time is modeled in the following equation 3 as an exponential relationship. Here the variable y gives the difference between the current and reference brightness temperatures, x is the time in minutes, A is a constant and the time constant is t, also expressed in minutes.

$$y = A * \exp(x/t) \tag{3}$$

It is seen from Fig. 4 that growth of the brightness temperature from reference value is exponential in nature. The regression analysis along with correlation coefficient, R^2=0.96 and time constant, t=7.24 are given in the figure legends. Another attempt is made to find out the rate of growth of the brightness temperature, that is, time constant of the exponential curve for different seasons, that is, by taking into account seasonal variation of the time constant.

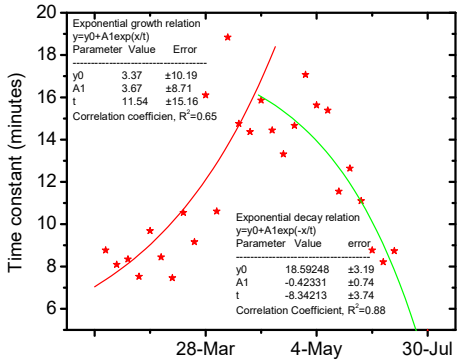

Fig. 5: Variation of the time constant of brightness temperature at 23.834 GHz for the year 2009

From Fig. 5 it is clear that as the monsoon activity increases, time constant is also increasing and attains its peak value at wettest period of the monsoon and again it is decreasing exponentially to the original brightness temperature.

Similar regression analyses of time constant are done here for pre-monsoon and post-monsoon period. The time constant is found to display a positive exponential growth for a particular period of time, after which it is found to decay exponentially. The equations 4 and 5 reflect the positive exponential growth and negative exponential decay respectively. For each equation, t_1 and t_2 represent the varying time constant values, t_{01} and t_{02} are the initial values of time constant for each of the time constant curves, A_1, A_2 and k_1, k_2 are constants and t_x is the time variation.

$$t_1 = t_{01} + A_1 * \exp(t_x/k_1) \quad (4)$$

$$t_2 = t_{02} + A_2 * \exp(-t_x/k_2) \quad (5)$$

From Fig. 5 is seen that during pre-monsoon period time constant growth is exponential in nature and reaches the peak value on 6th April, 2009 which is basically the peak of monsoon period in Brazil. Similarly in the post monsoon period it is showing exponential decay and attains the reference value of brightness temperature. The regression and correlation coefficients are illustrated in the figure legends.

A machine learning based linear spline regression method is proposed to generate an accurate estimate of the precursor time to a rain event, using the reference values of brightness temperatures at 23.834 GHz and 30 GHz and some of the corresponding precursor time values for rain events. Initially, the averages of brightness temperature value sets at 23.834 GHz and 30 GHz were used to divide each of the datasets into two parts. The corresponding regression spline equation sets are shown in the following Table 2.

Table 2:Spline regression equation sets for determination of rain precursor times at 23.834 GHz and 30 GHz

Reference value of T_B (K) at 23.834 GHz	Regression Equation Slope at 23.834 GHz	Regression Equation Intercept at 23.834 GHz	Reference value of T_B (K) at 30 GHz	Regression Equation Slope at 30 GHz	Regression Equation Intercept at 30 GHz
Up to 60.51	-0.066	37.439	Up to 31.47	0.446	26.701
Greater than 60.51	0.27	20.159	Greater than 31.47	0.401	25.334

The estimates obtained using the spline regression technique discussed above are compared with the actual precursor times. The results for 23.834 GHz and are shown in Fig. 6 and Fig. 7, which follow.

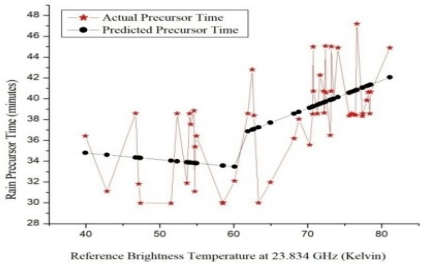

Fig. 6: Comparison of spline regression estimate rain precursor times with actual precursor times at 23.834 GHz

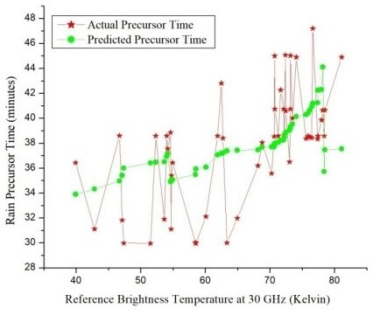

Fig. 7: Comparison of spline regression estimate rain precursor times with actual precursor times at 30 GHz

For increasing accuracy of prediction, two sets of spline regression equations are generated for 23.834 GHz and 30 GHz, based on monthly segmentation of data. The months of January and February have been combined in this analysis, since February witnessed only one rain event during the period of observation. The coefficients of the equations are shown in Table 3.

Table 3:Spline regression equations for monthly determination of rain precursor times at 23.834 GHz and 30 GHz

Month	Regression Equation Slope at 23.834 GHz	Regression Equation Intercept at 23.834 GHz	Regression Equation Slope at 30 GHz	Regression Equation Intercept at 30 GHz
January-February	0.232	21.345	0.175	32.512
March	-0.287	63.059	-0.272	50.734
April	0.241	26.367	0.272	34.032
May	0.009	37.862	0.009	38.144
June	-0.003	36.852	-0.092	38.595
July	0.004	30.669	0.028	30.185

The estimates obtained from application of spline regression to the month-wise segmented datasets for both frequencies are compared, as before, with the actual precursor times. The corresponding results are shown in Fig. 8 and Fig. 9 for reference brightness temperature values at 23.834 GHz and 30 GHz respectively.

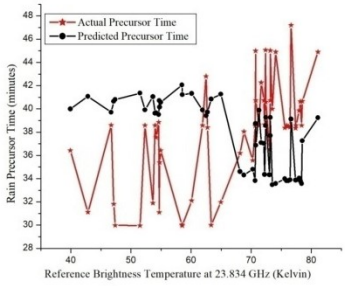

Fig. 8: Comparison of spline regression estimate rain precursor times from month-wise data with actual precursor times at 23.834 GHz

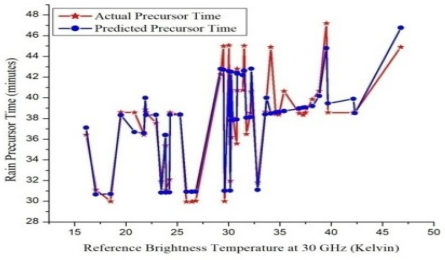

Fig. 9: Comparison of spline regression estimate rain precursor times from month-wise data with actual precursor times at 30 GHz

An average spline estimation was also performed using both of the month-wise segmented spline regression datasets, the result of which is shown in the following Fig. 10.

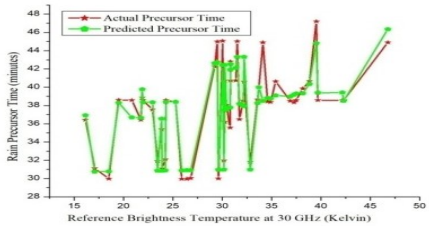

Fig. 10: Comparison of average spline regression estimate rain precursor times from month-wise data with actual precursor times

III. Results and Discussions

In the present work, the radiometric brightness temperature at two frequencies 23.834 and 30 GHz has been used for predicting the probability of occurrence of rain events. Amplitude of the time series of the brightness temperature rises at these two frequencies and rain rate shows the time gap between the thresholds and start of rain values varies from 29 to 47 minutes depending upon the nature of the rain event. This technique appears to be more acceptable because the initiation of rain is directly related to the presence of saturated water vapour and liquid water in the atmosphere which is reflected in the rise of brightness temperature at the selected frequency channels. This is an additional advantage that is obtained through use of brightness temperature as an observed parameter.

The reference brightness temperature data obtained at the frequencies of 23.834 GHz and 30 GHz has been used to propose machine learning based spline regression models that are more accurate than standard regression methods employed for prediction of rain precursor times. The initial spline regression models have been improved through the month-wise segmentation of data, which increases the accuracy of the proposed model by a considerable amount. This can be clearly observed by comparing between Fig. 6 and Fig. 8, for data at 23.834 GHz and Fig. 7 and Fig. 9, for 30 GHz.

It can also be seen that the estimates from the spline regression model for 23.834 GHz show a much greater variation from the actual values, compared to the estimates from the model at 30 GHz, which are much more accurate, as seen from Fig. 9. Finally, an average spline regression model using data from both 23.834 GHz and 30 GHz models has been used to estimate the actual rain precursor time values. The average spline model is better than both of the individual month-wise segment based spline models. However the estimates generated by this model are close to the estimates generated by the 30 GHz model with the maximum variation being 1 percent. Thus it can be concluded that these linear spline based models can be used to predict rainfall on a certain day from corresponding reference brightness temperature values.

IV. Conclusion

The variations observed during the course of the present work can be said to be indicators of rain initiation, as is evident from the results obtained by analyzing the available data. The threshold values found in this study can be further analyzed for evaluating different climatic situations especially in temperate climates to check the variability of the time interval before the initiation of precipitation.

The accuracy of predictions achieved by the current models can be further enhanced by applying other machine learning techniques such as SVM (Support Vector Machines). The authors intend to pursue further research in the present domain from these aspects.

References

I. Ahuna, M. N., Afullo, T. J. and Alonge, A. A., "Rain Attenuation Prediction Using Artificial Neural Network for Dynamic Rain Fade Mitigation," in SAIEE Africa Research Journal, vol. 110, no. 1, pp. 11-18, March 2019.

II. Barbaliscia, F., Fionda, E., &Masullo, P. G., “Ground-based radiometric measurements of atmospheric brightness temperature and water contents in Italy,” Radio Sci.,Vol. 33, no. 3,pp. 697-706, 1998.

III. Bosisio, A. V., Fionda, E., Basili, P., Carlesimo, G., Martellucci, A., “Identification of rainy periods from ground based microwave radiometry,” European Journal of Remote Sensing, Vol. 45, pp: 41-50, 2012.

IV. Bosisio, A. V., Fionda, E., Ciotti, P., Fionda, E., Martellucci, A., “Rainy events detection by means of observed brightness temperature ratio,” "Rainy events detection by means of observed brightness temperature ratio," 2012 12th Specialist Meeting on Microwave Radiometry and Remote Sensing of the Environment (MicroRad), Rome, pp. 1-4, 2012.

V. Chan, P.W., & Tam, C.M., “Performance and application of a multi-wavelength, ground-based microwave radiometer in rain now-casting”, 9th IOAS-AOLS of AMS., 2005.

VI. Chan, P.W., "Performance and application of a multi-wavelength, ground based microwave radiometer in intense convective weather," Meteorol. Z., Vol. 18, no.3,pp. 253–265, 2009.

VII. Chan, P.W., & Hon, K.K., "Application of ground-based, multichannel microwave radiometer in the now casting of intense convective weather through instability indices of the atmosphere," Meteorol. Z., Vol. 20, no.4, pp. 431–440, 2011.

VIII. Doran, J.C., Zhong, S., Liljegren, J. C., &Jakob, C., "A comparison of cloud properties at a coastal and inland site at the North Slope of Alaska," J. Geophys. Res.,Vol. 107 (D11), pp. 4120, doi:10.1029/2001JD000819., 2002.

IX. Dvorak, P., Mazanek, M., Zvanovec, S., "Short-term Prediction and Detection of Dynamic Atmospheric Phenomena by Microwave Radiometer," Radioengineering, Vol. 21, no. 4, Dec. 2012.

X. Geerts, B., "Estimating downburst-related maximum surface wind speeds by means of proximity soundings in New South Wales," Australia,Weather Forecast, Vol. 16, pp. 261–269, 2001.

XI. Güldner, J., &Spänkuch, D., "Results of year-round remotely sensed integrated water vapor by ground-based microwave radiometry", J. Appl. Meteorol., Vol. 38, pp:981-988, 1999.

XII. Güldner, J., &Spänkuch, D., "Remote sensing of the thermodynamic state of the atmospheric boundary layer by ground-based microwave radiometry," J. Atmos. Oceanic Technol., Vol. 18,pp: 925-933, 2001.

XIII. Hye, Y.W., Yeon-Hee, K., &Hee-Sang, L., "An application of brightness temperature received from a ground-based microwave radiometer to estimation of precipitation occurrences and rainfall intensity," Asia-Pacific Journal of Atmospheric Sciences, Vol. 45, no. 1, pp: 55-69, 2009.

XIV. Karmakar, P. K., Maiti, M., Calheiros, A. J. P., Angelis, C. F., Machado, L. A. T., Da Costa, S. S., "Ground based single frequency micro -wave radiometric measurement of water vapour ," International Journal of remote sensing(UK) , vol. 32, No. 23, pp 1-11, 2011.

XV. Knupp, K., Ware, R., Cimni, D., Vandenberghe F., Vivekanandan, J., Westwater, E., Coleman, T., "Ground-based passive microwave profiling during dynamic weather conditions," J. Atmos. Oceanic Technol., Vol. 26, pp. 1057–1072, 2009.

XVI. Liu, G. R., "Rainfall intensity estimation by ground-based dual-frequency microwave radiometers," Journal of Applied Meteorology, Vol. 40, pp: 1035-1041, 2001.

XVII. Lee, O.S.M., "Forecast of strong gusts associated with thunderstorms based on data from radiosonde ascents and automatic weather stations in China", 21st Guangdong–Hong Kong–Macao Technical Seminar on Meteorological Science and Technology, Hong Kong, 24–26 Jan. 2007.

XVIII. Madhulatha, A., Rajeevan, M., Ratnam, M. Venkat, Bhate, Jyoti, & Naidu, C. V., "Now casting severe convective activity over southeast India using ground-based microwave radiometer observations," Journal of Geophysical Research, Vol. 118, pp.1-13, 2013.

XIX. Manandhar, S., Lee, Y. H., Meng, Y. S., Yuan, F. and Ong, J. T., "GPS-Derived PWV for Rainfall Nowcasting in Tropical Region," in IEEE Transactions on Geoscience and Remote Sensing, vol. 56, no. 8, pp. 4835-4844, Aug. 2018.

XX. Manzato, A., "A climatology of instability indices derived from Friuli Venezia Giulia soundings, using three different methods," Atmos. Res., 67–68, 417–454, 2003.

XXI. McCann, D. W., "WINDEX—A new index for forecasting microburst potential," Weather Forecast, Vol. 9, pp. 532–541, 1994.

XXII. Ojo, J. S., Ajewole, M. O., &Sarkar, S. K., "Rain Rate Attenuation Prediction for Satellite communication in Ku and Ka Bands over Nigeria," Progress In Electromagnetics Research B, Vol. 5, 207–223, 2008.

XXIII. Qiu, Minghui, Zhao, Peilin, Zhang, Ke, Huang, Jun, Shi, Xing, Wang, Xiaoguang& Chu, Wei, "A Short-Term Rainfall Prediction Model Using Multi-task Convolutional Neural Networks," 2017 IEEE International Conference on Data Mining (ICDM), New Orleans, LA, 2017, pp. 395-404.

XXIV. Rivero, C. Rodriguez, Pucheta, J., Herrera, M., Sauchelli, V. and Laboret, S., "Time Series Forecasting Using Bayesian Method: Application to Cumulative Rainfall," in IEEE Latin America Transactions, vol. 11, no. 1, pp. 359-364, Feb. 2013.

XXV. Rose, T. &Czekala H.," Filter bank radiometers for atmospheric profiling," Sixth International Symposium on Tropospheric Profiling: Needs and Technologies. Meckenhiem, Germany, 2003.

XXVI. Ulaby, F. T., Moore, R. K., Fung, A. K., "Microwave Remote Sensing Active and Passive," Vol. 1, Microwave Remote Sensing Fundamentals and Radiometry, Addison-Wesley, 1981.

XXVII. Ware, R., Solheim, F., Carpenter, R., Gueldner, J., Liljegren, J., Nehrkorn, T., &Vandenberghe, F., "A multi-channel radiometric profiler of temperature, humidity and cloud liquid," Radio Sci., vol. 38, no. 4, 8079, pp.1–13, 2003.

XXVIII. Yang, H.Y., Chang, K.H., & Oh, S. N., "Measurements of precipitable water vapor and liquid water path by dual-channel microwave radiometer during 2001-2003," Proceedings of the Autumn Meeting of KMS, 104-105, 2006.

XXIX. Zhang, Pengcheng, Jia, Yangyang, Gao, Jerry, Song, Wei, and Leung, Hareton K. N., "Short-term Rainfall Forecasting Using Multi-layer Perceptron," in IEEE Transactions on Big Data, 2018.